Analytica Chimica Acta 800 (2013) 71–76

Contents lists available at ScienceDirect

Analytica Chimica Acta

journal homepage: www.elsevier.com/locate/aca

Hypochlorous acid turn-on boron dipyrromethene probe based on oxidation of methyl phenyl sulfide

Shi-Rong Liu, Mani Vedamalai, Shu-Pao Wu*

Department of Applied Chemistry, National Chiao Tung University, Hsinchu, Taiwan 300, Republic of China

HIGHLIGHTS

- A BODIPY-based green fluorescent probe for sensing HOCl was developed.
- The probe utilizes HOCl-promoted oxidation of methyl phenyl sulfide to produce a proportional fluorescence response to the concentration of HOCl.
- Confocal fluorescence microscopy imaging of RAW264.7 cells demonstrated that the **HCS** probe might have application in the investigation of HOCl roles in biological systems.

GRAPHICAL ABSTRACT

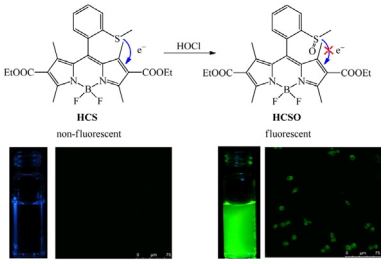

ARTICLE INFO

Article history:
Received 9 April 2013
Received in revised form 19 August 2013
Accepted 6 September 2013
Available online 12 September 2013

Keywords:
Hypochlorous acid
Fluorescent probe
Boron dipyrromethene
Bioimaging

ABSTRACT

A boron dipyrromethene (BODIPY)-based fluorometric probe, **HCS**, has been successfully developed for the highly sensitive and selective detection of hypochlorous acid (HOCl). The probe is based on the specific HOCl-promoted oxidation of methyl phenyl sulfide. The reaction is accompanied by a 160-fold increase in the fluorescent quantum yield (from 0.003 to 0.480). The fluorescent turn-on mechanism is accomplished by suppression of photoinduced electron transfer (PET) from the methyl phenyl sulfide group to BODIPY. The fluorescence intensity of the reaction between HOCl and **HCS** shows a good linearity in the HOCl concentration range 1–10 μM. The detection limit is 23.7 nM (S/N = 3). In addition, confocal fluorescence microscopy imaging using RAW264.7 macrophages demonstrates that the **HCS** probe could be an efficient fluorescent detector for HOCl in living cells.

1. Introduction

Hypochlorous acid (HOCl), one of the reactive oxygen species (ROS), is a highly effective antimicrobial agent used by mammalian immune systems [1]. Endogenous HOCl is produced from the reaction between hydrogen peroxide and chloride ion, which is catalyzed by myeloperoxidase (MPO) [2] in leukocytes, including macrophages, monocytes and neutrophils [3]. When pathogens invade human tissue, leukocytes engulf the invading pathogens by phagocytosis. Endogenous HOCl can damage various biomolecules, including DNA, lipids, and proteins, and then kill the invading pathogens [4]. However, uncontrolled HOCl production can result in the emergence of diseases, including atherosclerosis [5], atrial fibrillation [6], and liver cirrhosis [7]. Because of the biological importance of HOCl, the development of highly sensitive and selective probes for HOCl is an important issue. Fluorescent probes that can respond to changes in the concentration of HOCl would be helpful in studying the dynamic distribution of HOCl in living cells [8–25].

* Corresponding author. Tel.: +886 3 5712121x56506; fax: +886 3 5723764.
E-mail addresses: spwu@mail.nctu.edu.tw, spwu@faculty.nctu.edu.tw (S.-P. Wu).

0003-2670/$ – see front matter © 2013 Published by Elsevier B.V.
http://dx.doi.org/10.1016/j.aca.2013.09.018

A common strategy for the design of HOCl fluorescent probes is to connect a HOCl-reactive moiety to an organic fluorophore. The HOCl-reactive component functions as a controller that modulates the fluorescence intensity of the fluorophore by a photoinduced electron transfer (PET) mechanism. In the absence of HOCl, the fluorescence of the fluorophore is quenched by the PET process; however, in the presence of HOCl, PET quenching is restricted and fluorescence of the fluorophore is reestablished. To facilitate the practical application of HOCl probes in cell imaging, HOCl probe development has focused on selectivity and sensitivity. Herein, we report a highly sensitive and selective fluorescent probe for HOCl that is based on the HOCl-promoted oxidation of methyl phenyl sulfide.

In this study, we designed a new boron dipyrromethene (BODIPY)-based fluorescent probe, **HCS**, containing an organosulfur group for HOCl detection. BODIPY is a fluorescent dye with a large molar absorption coefficient and high fluorescence quantum yield [26]. We used BODIPY as the signal transducer and methyl phenyl sulfide as the modulator that responds to the amount of HOCl. **HCS** produces weak fluorescence with a quantum yield of $\Phi = 0.003$ in response to PET from the methyl phenyl sulfide group to BODIPY. However, BODIPY produces strong fluorescence upon oxidation of sulfur by HOCl. The probe exhibits greater selectivity and sensitivity toward HOCl than it does for other ROS and reactive nitrogen species (RNS) in aqueous solution. Importantly, **HCS** has good cell-membrane permeability and can successfully image HOCl in living cells.

2. Experimental

2.1. Materials and instrumentation

All reagents were obtained from commercial sources and used as received without further purification. UV/vis spectra were recorded on an Agilent 8453 UV/vis spectrometer. Fluorescence spectra measurements were performed on a Hitachi F-7000 fluorescence spectrophotometer. NMR spectra were obtained on a Bruker DRX-300 and Agilent Unity INOVA-500 NMR spectrometer. Fluorescent images were taken on a Leica TCS SP5 X AOBS Confocal Fluorescence Microscope.

2.2. Preparation of ROS and RNS

Various ROS and RNS including HOCl, •OH, H_2O_2, $^1O_2$, NO_2^-, NO_3^-, NO, $ONOO^-$, O_2^- and *t*-BuOOH were prepared according to the following methods. HOCl was prepared from commercial bleach; the concentration of hypochlorite (OCl^-) was determined by using an extinction coefficient of $350\,M^{-1}\,cm^{-1}$ (292 nm) at pH 9.0. Hydroxyl radical (•OH) was generated by Fenton reaction on mixing $Fe(NH_4)_2(SO_4)_2{\cdot}6H_2O$ with 10 equivalents of H_2O_2; the concentration of •OH was estimated from the concentration of Fe^{2+}. The concentration of the commercially available stock H_2O_2 solution was estimated by optical absorbance at 240 nm. Singlet oxygen ($^1O_2$) was generated by the addition of NaOCl and H_2O_2 according to the literature [27]. The source of NO_2 and NO_3 was from $NaNO_2$ and $NaNO_3$. Nitric oxide (NO) was generated from SNP (Sodium Nitroferricyanide (III) Dihydrate). Peroxynitrite ($ONOO^-$) was prepared as the reported method[2]; the concentration of peroxynitrite was estimated by using an extinction coefficient of $1670\,M^{-1}\,cm^{-1}$ (302 nm). Superoxide (O_2^-) is prepared from KO_2. *t*-BuOOH was obtained commercially from Alfa Aesar.

2.3. Synthesis of **HCS**

TFA (0.1 mL) was added to the solution of 2-methylthiobenzaldehyde (516 μL, 4 mmol) and ethyl 2,4-dimethyl-1H-pyrrole-3-carboxylate (762 mg, 8.00 mmol) in 150 mL of CH_2Cl_2 under N_2 atmosphere. After the solution was stirred for three hours, TLC analysis revealed complete conversion of starting materials to the dipyrromethane. To the reaction mixture, DDQ (953.4 mg, 4.20 mmol) dissolved in CH_2Cl_2 was added. Then, the solution was stirred for further 45 min; TLC analysis revealed the complete disappearance of dipyrromethane and formation of the desired dipyrromethene. Triethylamine (4.0 mL) and boron trifluoride diethetate (4.0 mL) were added to the reaction mixture and stirring was continued for further 2 h. Reaction mixture was washed with water (50 mL) by three times and the organic phase was dried over anhydrous $MgSO_4$. The solvent was removed under reduced pressure and the crude product was purified by column chromatography (hexane: dichloromethane = 8:1) to give the compound **HCS** as an orange solid. Yield: 493.6 mg (24%); m.p. 241–242 °C. ^{1}H NMR (300 MHz, $CDCl_3$) $\delta = 7.51$ (t, $J = 8.1$ Hz, 1H), 7.26–7.34 (m, 2H), 7.12 (d, $J = 7.2$ Hz, 1H), 4.27 (q, $J = 7.2$ Hz, 4H), 2.84 (s, 6H), 2.44 (s, 3H), 1.78 (s, 6H), 1.32 (t, $J = 7.2$ Hz, 6H). ^{13}C NMR (75 MHz, $CDCl_3$) $\delta = 164.2$, 159.6, 147.2, 143.5, 137.9, 132.1, 130.9, 130.3, 128.0, 125.8, 125.1, 122.2, 60.1, 15.0, 14.9, 14.2, 12.7. MS (EI): *m*/*z* (%) = 514 (100), 469 (17), 468 (19), 467 (14), 447 (31), 440 (10), 421 (10), 420 (9), 394 (8), 393 (12), 392 (9), 375 (10), 374 (16), 373 (13). HRMS (EI): calcd. for $C_{26}H_{29}BF_2N_2O_4S$ 514.1909, found 514.1916. FTIR (cm^{-1}) 1703, 1518, 1434, 1313, 1253, 1180, 1113, 1029.

2.4. The oxidized product (**HCSO**) from the reaction of **HCS** and NaOCl

NaOCl (530 μL, 12% dissolved in H_2O) was added to the solution of **HCS** (257.1 mg, 0.5 mmol) in CH_3CN (50 mL). The reaction mixture was stirred at room temperature for 30 min. The solvent was evaporated under reduced pressure, and the crude product was purified by column chromatography using ethyl acetate and hexane as eluents (1:6, v/v) to give the compound **HCSO** as dark red solid. Yield: 137.8 mg (52%); m.p. 232–233 °C. ^{1}H NMR (300 MHz, $CDCl_3$) 8.27 (dd, $J = 8.1$ Hz, $J = 0.9$ Hz, 1H), 7.85 (td, $J = 7.7$, $J = 1.2$ Hz, 1H), 7.70 (td, $J = 7.5$ Hz, $J = 1.2$ Hz, 1H), 7.32 (dd, $J = 7.5$ Hz, $J = 0.9$ Hz, 1H), 4.27 (m, 4H), 2.86 (s, 3H), 2.84 (s, 3H), 2.59 (s, 3H), 1.71 (s, 3H), 1.60 (s, 3H), 1.33 (m, 6H). ^{13}C NMR (150 MHz, $CDCl_3$) δ 163.9, 163.8, 161.8, 159.8, 148.0, 145.4, 144.5, 139.9, 132.2, 131.8, 131.6, 130.8, 128.7, 125.3, 123.5, 122.7, 60.43, 60.37, 42.3, 15.2, 15.0, 14.21, 14.18, 13.7, 13.4. MS (ESI): *m*/*z* 531.0. HRMS (ESI): calcd. for $C_{26}H_{29}BF_2N_2O_5S$ 530.1858, found 530.1856. FTIR (cm^{-1}) 1710, 1547, 1443, 1320, 1247, 1188, 1109, 1073, 1031.

2.5. Cell culture for RAW264.7 macrophages

The cell line RAW264.7 was provided by the Food Industry Research and Development Institute (Taiwan). RAW264.7 cells were cultured in Dulbecco's Modified Eagle's medium (DMEM) supplemented with 10% fetal bovine serum (FBS) at 37 °C under an atmosphere of 5% CO_2. Cells were plated on 18 mm glass coverslips and allowed to adhere for 24 h.

2.6. Fluorescence imaging of exogenous HOCl in living cells

Experiments to assess the sensing ability of **HCS** for exogenous HOCl were performed in 0.1 M phosphate-buffered saline (PBS) with NaOCl (10 μM). Treat the cells with 2 μL of 10 mM **HCS** (final concentration: 10 μM) dissolved in DMSO and incubated for 30 min at 37 °C. The treated cells were washed with 0.1 M PBS

(2 mL × 3) to remove remaining **HCS**. DMEM (2 mL) was added to the cell culture, which was then treated with 10 mM solution of NaOCl (2 μL; final concentration: 10 μM) dissolved in sterilized 0.1 M PBS (pH 7.4). The samples were incubated at 37 °C for 10 min. The culture medium was removed, and the treated cells were washed with 0.1 M PBS (2 mL × 3) before observation. Confocal fluorescence imaging of cells was performed with a Leica TCS SP5 X AOBS Confocal Fluorescence Microscope (Germany), and a 63× oil-immersion objective lens was used. The cells were excited with a white light laser at 488 nm, and emission was collected at 530 ± 10 nm.

2.7. Fluorescence imaging of PMA-induced HOCl production in living cells

RAW264.7 cells were treated with PMA (25 ng mL^{-1}) and **HCS** in culture medium for 2 h. The culture medium was removed, and the treated cells were washed with 0.1 M PBS (2 mL × 3) before observation. Fluorescence imaging was performed with a Leica TCS SP5 X AOBS Confocal Fluorescence Microscope. The cells were excited with a white light laser at 488 nm, and emission was collected at 530 ± 10 nm.

2.8. Quantum chemical calculation

Quantum chemical calculations based on density functional theory (DFT) were carried out using a Gaussian 09 program. The optimized geometries and energy levels of frontier molecular orbitals were performed using the B3LYP functional and the 6-31G basis set.

3. Results and discussion

3.1. Synthesis of the probe *HCS*

The synthetic procedure for the probe **HCS** is outlined in Scheme 1. Treatment of 2-(methylthio)benzaldehyde with ethyl 2,4-dimethyl-1H-pyrrole-3-carboxylate in the presence of trifluoroacetic acid (TFA) under N_2 produces the corresponding dipyrromethane. In the following step, 2-(methylthio)phenyldipyrromethane is oxidized with 2,3-dichloro-5,6-dicyano-1,4-benzoquinone (DDQ) to produce the corresponding dipyrromethene, which is then transformed into the BODIPY skeleton in the presence of BF_3. The structures of **HCS** and of **HCSO**, the product of the reaction of **HCS** with HOCl, were confirmed using ^{1}H and ^{13}C NMR spectroscopy and mass spectrometry. **HCS** has an absorbance maximum at 546 nm, assigned to the $S_0 \rightarrow S_1$ transition of the BODIPY chromophore [26], and a molar extinction coefficient of 2.42×10^4 m^{-1}cm^{-1}. **HCS** displays weak fluorescence with a quantum yield of $\Phi = 0.003$, because photoinduced electron transfer from the aromatic sulfur group to the BODIPY moiety takes place.

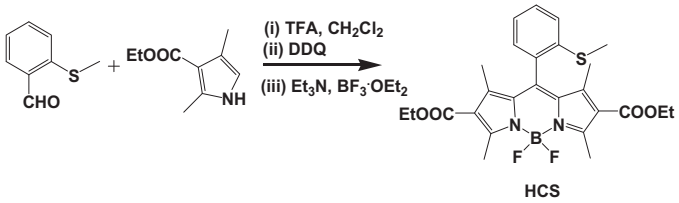

Scheme 1. Synthesis of the probe **HCS**.

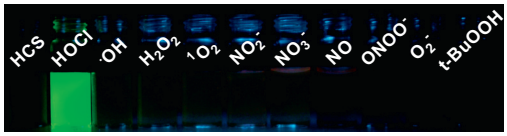

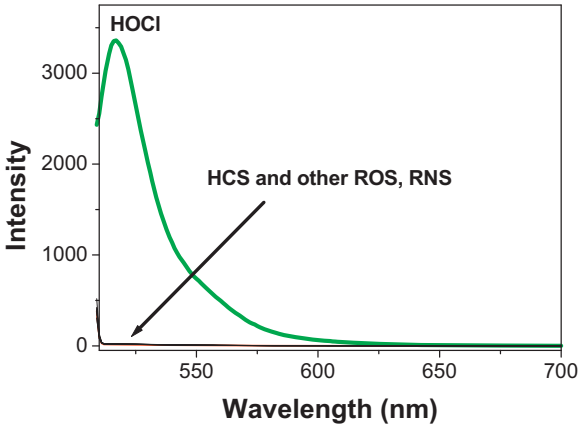

Fig. 1. Fluorescence changes in **HCS** (10 μM) in response to treatment with NaOCl (20 μM) and various ROS/RNS (100 μM) in a water–CH_3CN solution.

3.2. Fluorescent response of *HCS* with HOCl

We tested the sensing performance of the **HCS** probe toward various ROS and RNS species, including HOCl, •OH, H_2O_2, $^1O_2$, NO_2^-, NO_3^-, NO, $ONOO^-$, O_2^-, and *t*-BuOOH, in phosphate-buffered saline (PBS) solution. We found that strong green fluorescence only occurred upon addition of HOCl to a solution containing **HCS**; other ROS and RNS produced no change in fluorescence (Fig. 1). Quantitative **HCS** fluorescence was observed in the presence of several ROS and RNS that we tested, but HOCl was the only reactive species that caused significant fluorescence enhancement.

To study the influence of other ROS/RNS on the reaction of **HCS** with HOCl, competitive experiments were performed with other ROS/RNS (100 μM) in the presence of NaOCl (20 μM). In Fig. 2, the fluorescence enhancement caused by mixing NaOCl with most ROS/RNS was similar to that caused by NaOCl alone. Smaller fluorescence intensity was observed only when NaOCl was mixed with H_2O_2. NaOCl can react with H_2O_2 to furnish $^1O_2$ [27], which shows no response toward probe **HCS**. Due to the consumption of NaOCl by H_2O_2, smaller fluorescence intensity was observed in the

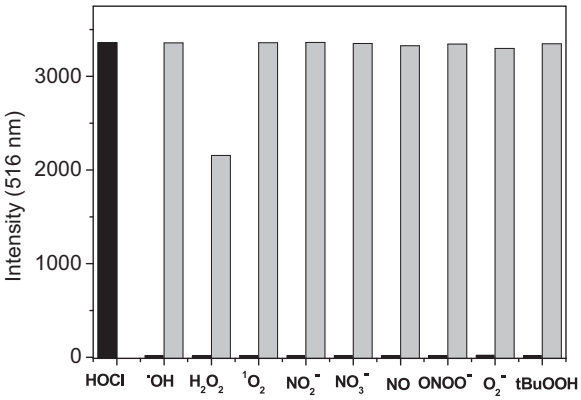

Fig. 2. Fluorescence response (516 nm) of probe **HCS** (10 μM) to NaOCl (20 μM) or 100 μM of other ROS/RNS (the black bar portion) and to the mixture of other ROS/RNS (100 μM) with 20 μM of NaOCl (the gray bar portion) in a water–CH_3CN solution (v/v = 99/1, 0.1 M PBS, pH 7.4). The excitation wavelength was 505 nm.

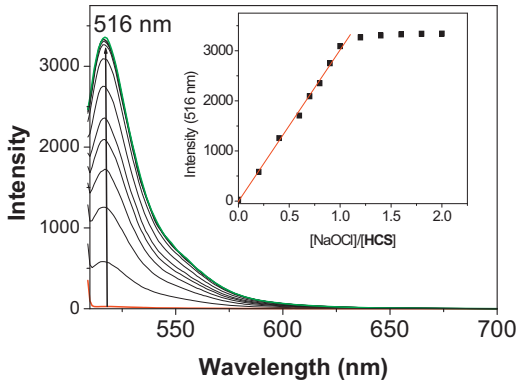

Fig. 3. Fluorescence changes in **HCS** (10 μM) in the presence of various equivalents of NaOCl in a water–CH_3CN solution. The excitation wavelength was 505 nm.

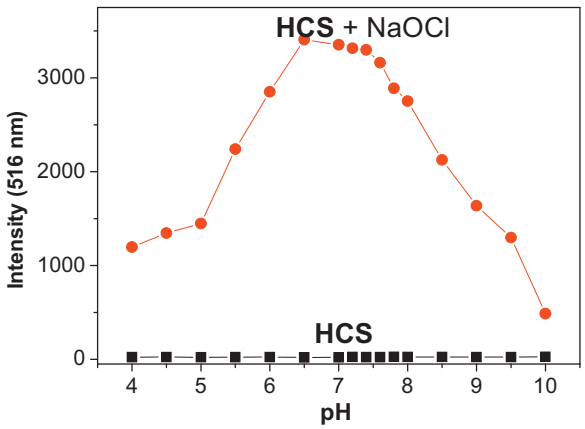

Fig. 4. Fluorescence response (516 nm) of free probe **HCS** (10 μM), and fluorescence response after addition of NaOCl (20 μM) to a H_2O–CH_3CN solution (v/v = 99/1, 0.1 M PBS buffer) as functions of pH value. The excitation wavelength was 505 nm.

presence of NaOCl and H_2O_2. To further evaluate the selectivity of the probe **HCS** toward HOCl, 15 different metal ions (Ag^+, Al^{3+}, Ca^{2+}, Cd^{2+}, Co^{2+}, Cr^{3+}, Cu^{2+}, Fe^{2+}, Fe^{3+}, Hg^{2+}, Mg^{2+}, Mn^{2+}, Ni^{2+}, Pb^{2+}, Zn^{2+}) and 10 different anions (Br^-, CH_3COO^-, ClO_4^-, CN^-, F^-, HSO_4^-, HPO_4^{2-}, $H_2PO_4^-$, I^-, SCN^-) were tested. No ion showed any noticeable change in fluorescence intensity (Fig. S7 and Fig. S8), indicating no response toward the probe **HCS**. This result suggested that **HCS** can respond to HOCl with low interference.

The reaction of **HCS** with HOCl is fast; addition of NaOCl(aq) to a solution containing **HCS** results in an immediate strong increase in fluorescence intensity (Fig. S5 in the Supporting Information). During HOCl titration with **HCS**, a new emission band appeared at 516 nm (Fig. 3). The emission intensity reached its maximum after the addition of one equivalent of HOCl. The quantum yield of the oxidized form, **HCSO**, was $\Phi = 0.480$, which is 160-fold greater than that of **HCS** (0.003). The structure of **HCSO** was confirmed by ^1H NMR, ^{13}C NMR, and MS spectrometry. We observed a good linear correlation between fluorescence intensity and HOCl concentration over the range 0–10 μM, and found that **HCS** has a detection limit of 23.7 nM (Fig. S6 in the Supporting Information), indicating that it is sufficiently sensitive for detection of HOCl in living systems.

Density functional theory (DFT) calculation was applied to determine the HOCl-detection mechanism. As shown in Scheme 2, the highest occupied molecular orbital (HOMO) of the methyl phenyl sulfide moiety (electron donor) is close to that of the fluorophore BODIPY (electron acceptor); the HOMO energy level (−5.57 eV) of the methyl phenyl sulfide moiety is higher than that of BODIPY (−5.81 eV). Consequently, when the BODIPY moiety is excited by light, the electron transfer from the methyl phenyl sulfide moiety to the BODIPY moiety is energetically allowed. Hence, the BODIPY fluorescence is quenched by the PET process ($\Phi < 0.01$). In contrast, upon the oxidation of **HCS** by HOCl, the HOMO energy level of the methyl phenyl sulfoxide moiety (−5.95 eV) is below that of BODIPY; thus, the PET process is forbidden and BODIPY fluorescence reemerges [26].

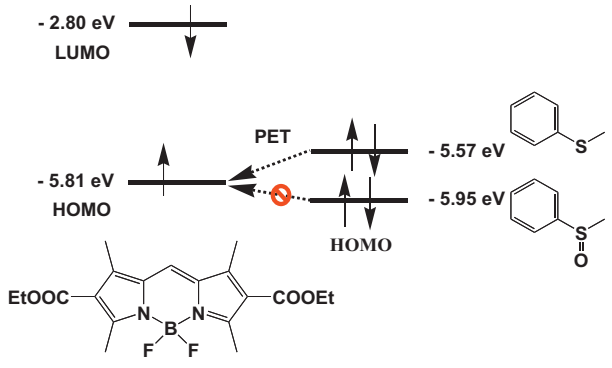

Scheme 2. Energy diagram for the reaction of **HCS** with HOCl.

A pH-dependence experiment of **HCS** was conducted to determine a suitable pH range for HOCl sensing. Fig. 4 shows that the **HCS** emission intensity is very low over the range pH 4–10. After addition of one equivalent of HOCl, the emission intensity at 516 nm significantly increases over the pH range 5.5–8.0, indicating that the probe is suitable for use under physiological conditions. At pH values greater than 8.5, the emission intensity decreases sharply. This occurs because the pK_a of HOCl is 7.6 [8,11]; hypochlorite (ClO^-) is dominant at pH > 8, and has low reactivity with **HCS**.

3.3. *Bioimaging of **HCS***

The potential of the probe **HCS** for imaging HOCl in living cells was next investigated. RAW264.7 macrophages were used as a model cell line because macrophages are known to generate ROS and RNS in the immune system. Images of cells were obtained using confocal fluorescence microscopy. No fluorescence was observed for RAW264.7 cells that were incubated with 10 μM **HCS** (Fig. 5a). After treatment with NaOCl, bright green fluorescence was observed in the RAW264.7 cells (Fig. 5b). The overlay of fluorescence and bright-field images reveal that the fluorescence signals are localized in the intracellular area, indicating a subcellular distribution of HOCl and good **HCS** cell-membrane permeability.

Furthermore, **HCS** was used to detect PMA-induced endogenous HOCl production in RAW264.7 cells. Phorbol myristate acetate (PMA) activates the generation of ROS and RNS, including HOCl, in macrophage cells [28,29]. After stimulation with PMA (25 ng mL^{-1}) for 2 h in the presence of **HCS**, strong green fluorescence was observed in the RAW264.7 cells (Fig. 5c). These results demonstrate that **HCS** can visualize PMA-induced endogenous HOCl production in macrophages. When the MPO inhibitor 4-aminobenzoic acid hydrazide (ABAH, 100 μM) was added together with PMA (25 ng mL^{-1}) to macrophage cells, no fluorescence enhancement was observed. These results demonstrate that only the presence of HOCl results in significant fluorescence enhancement in cells, whereas other ROS and RNS produce insignificant fluorescence enhancement.

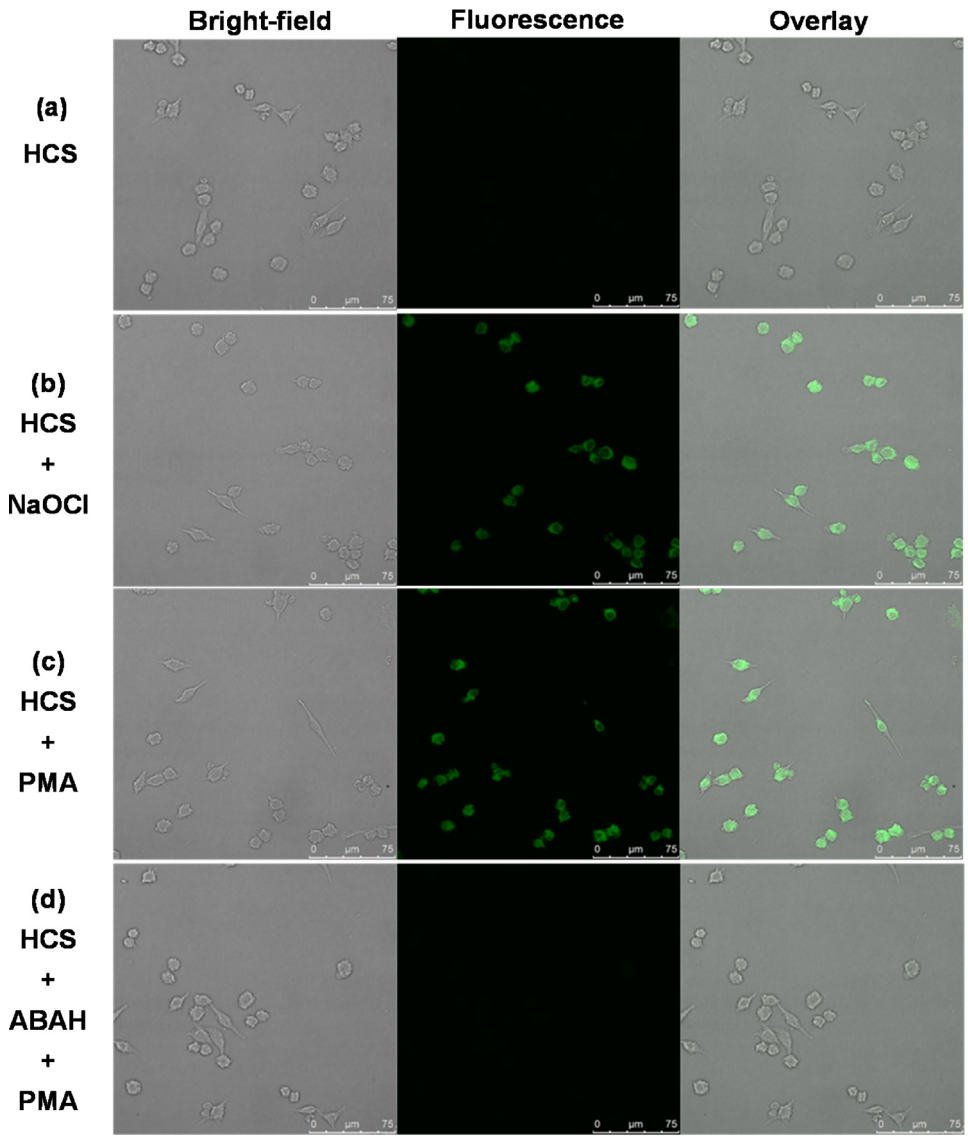

Fig. 5. Fluorescence images of RAW264.7 cells. (Left) Bright-field image; (Middle) fluorescence image; and (Right) merged image. (a) The cells incubated with **HCS** (10 μM) for 30 min at 37 °C. (b) The cells loaded with **HCS** (10 μM), incubated with NaOCl (10 μM) for 1 h at 37 °C. (c) The cells treated with PMA (25 ng mL^{-1}) for 2 h at 37 °C in the presence of **HCS** (10 μM). (d) ABAH (100 μM) was co-incubated with **HCS** (10 μM) for 1 h at 37 °C during PMA stimulation.

4. Conclusion

In summary, we developed a BODIPY-based green fluorescent probe, **HCS**, which produces a rapid, highly selective, and sensitive response to HOCl, but not to other reactive species. The probe utilizes HOCl-promoted oxidation of methyl phenyl sulfide to produce a proportional fluorescence response to the concentration of HOCl. Confocal fluorescence microscopy imaging of RAW264.7 cells demonstrated that the **HCS** probe might have application in the investigation of HOCl roles in biological systems.

Acknowledgments

We gratefully acknowledge the financial support of the National Science Council (ROC) and National Chiao Tung University.

Appendix A. Supplementary data

Supplementary data associated with this article can be found, in the online version, at http://dx.doi.org/10.1016/j.aca.2013.09.018.

References

[1] C.C. Winterbourn, M.B. Hampton, J.H. Livesey, A.J. Kettle, J. Biol. Chem. 281 (2006) 39869.
[2] T.J. Fiedler, C.A. Davey, R.E. Fenna, J. Biol. Chem. 275 (2000) 119671.
[3] Y.W. Yap, M. Whiteman, N.S. Cheung, Cell. Signal. 19 (2007) 228.
[4] D.I. Pattison, M.J. Davies, Chem. Res. Toxicol. 14 (2001) 1464.
[5] L.J. Hazell, L. Arnold, D. Flowers, G. Waeg, E. Malle, R. Stocker, J. Clin. Invest. 97 (1996) 1544.
[6] V. Rudolph, R.P. Andrie, T.K. Rudolph, K. Friedrichs, A. Klinke, B. Hirsch-Hoffmann, A.P. Schwoerer, D. Lau, X.M. Fu, K. Klingel, K. Sydow, M. Didie, A. Seniuk, E.C. von Leitner, K. Szoecs, J.W. Schrickel, H. Treede, U. Wenzel, T. Lewalter, G. Nickenig, W.H. Zimmermann, T. Meinertz, R.H. Boger, H. Reichenspurner, B.A. Freeman, T. Eschenhagen, H. Ehmke, S.L. Hazen, S. Willems, S. Baldus, Nat. Med. 16 (2010) 475.
[7] M. Whiteman, P. Rose, J.L. Siau, N.S. Cheung, G.S. Tan, B. Halliwell, J.S. Armstrong, Free Radic. Biol. Med. 38 (2005) 1584.
[8] S. Kenmoku, Y. Urano, H. Kojima, T. Nagano, J. Am. Chem. Soc. 129 (2007) 7318.
[9] Y. Koide, Y. Urano, S. Kenmoku, H. Kojima, T. Nagano, J. Am. Chem. Soc. 129 (2007) 10325.
[10] X. Chen, X. Wang, S. Wang, W. Shi, K. Wang, H. Ma, Chem. Eur. J. 14 (2008) 4724.
[11] Z. Sun, F. Liu, Y. Chen, P.K.H. Tam, D. Yang, Org. Lett. 10 (2008) 2174.
[12] Y. Yang, H.J. Cho, J. Lee, I. Shin, J. Tae, Org. Lett. 11 (2009) 861.
[13] W. Lin, L. Long, B. Chen, W. Tan, Chem. Eur. J 15 (2009) 2309.
[14] P. Panizzi, M. Nahrendorf, M. Wildgruber, P. Waterman, J.L. Figueiredo, E. Aikawa, J. McCarthy, R. Weissleder, S.A. Hilderbrand, J. Am. Chem. Soc. 131 (2009) 15744.

[15] K. Cui, D.Q. Zhang, G.X. Zhang, D.B. Zhu, Tetrahedron Lett. 51 (2010) 6055.
[16] X.D. Lou, Y. Zhang, Q.Q. Li, J.G. Qin, Z. Li, Chem. Commun. 47 (2011) 3191.
[17] X. Cheng, H. Jia, T. Long, J. Feng, J. Qin, Z. Li, Chem. Commun. 47 (2011) 11980.
[18] Y. Koide, Y. Urano, K. Hanaoka, T. Terai, T. Nagano, J. Am. Chem. Soc. 133 (2011) 5682.
[19] Y. Zhou, J. Li, K. Chu, K. Liu, C. Yao, J. Li, Chem. Commun. 48 (2012) 4679.
[20] G. Chen, F. Song, J. Wang, Z. Yang, S. Sun, J. Fan, X. Qiang, X. Wang, B. Dou, X. Peng, Chem. Commun. 48 (2012) 2951.
[21] S. Liu, S. Wu, Org. Lett. 15 (2013) 881.
[22] B. Wang, P. Li, F. Yu, P. Song, X. Sun, S. Yang, Z. Lou, K. Han, Chem. Commun. 49 (2013) 1016.
[23] L. Gai, J. Mack, H. Liu, Z. Xu, H. Lu, Z. Li, Sens. Actuators B 182 (2013) 6.
[24] L. Long, D. Zhang, X. Li, J. Zhang, C. Zhang, L. Zhou, Anal. Chim. Acta 775 (2013) 105.
[25] Q. Xu, K. Lee, S. Lee, K.M. Lee, W. Lee, J. Yoon, J. Am. Chem. Soc. 135 (2013) 9949.
[26] A. Loudet, K. Burgess, Chem. Rev. 107 (2007) 4932.
[27] X.H. Li, G.X. Zhang, H.M. Ma, D.Q. Zhang, J. Li, D.B. Zhu, J. Am. Chem. Soc. 126 (2004) 11548.
[28] M. Wolfson, L.C. McPhail, V.N. Nasrallah, R. Snyderman, J. Immunol. 135 (1985) 2062.
[29] Y. Yang, H. Lu, W. Wang, I. Liau, Anal. Chem. 83 (2011) 8272.